

Supporting Information

An Isolable Bismabenzene: Synthesis, Structure, and Reactivity

Takuya Ishii, Katsunori Suzuki,* Taichi Nakamura, and Makoto Yamashita*

*Department of Applied Chemistry, Faculty of Science and Engineering, Chuo University,
1-13-27 Kasuga, Bunkyo-ku, 112-8551, Japan*

E-mail: katsuno_suzu@oec.chem.chuo-u.ac.jp; makoto@oec.chem.chuo-u.ac.jp

Contents

1.	Experimental procedures	S2
2.	X-ray crystallographic analysis	S5
3.	UV-vis absorption spectrum	S10
4.	Theoretical calculations	S11
5.	References	S18

1. Experimental Procedures

General methods

All manipulations of air- and/or moisture-sensitive compounds were performed either using standard Schlenk-line techniques or in glovebox (MIWA and KOREA KIYON) under inert atmosphere of argon. Anhydrous hexane, toluene, and diethylether (Et_2O) were dried by passage through a GrassContour solvent purification system. Deuterated chloroform (CDCl_3) was distilled from CaH_2 prior to use. Deuterated benzene (C_6D_6) was distilled from sodium/benzophenone prior to use. Aluminacyclohexadiene **2** was prepared according to the literature procedure.^{S1} Other chemicals were used as received. The nuclear magnetic resonance (NMR) measurements were carried out by a JEOL ECA-500 spectrometer (500 MHz for ^1H , and 126 MHz for ^{13}C) or a JEOL ECS-400 spectrometer (400 MHz for ^1H and 100 MHz for ^{13}C). Chemical shifts (δ) are given by definition as dimensionless numbers and relative to ^1H and ^{13}C NMR chemical shifts of the residual CHCl_3 for ^1H ($\delta = 7.26$) and CDCl_3 itself for ^{13}C ($\delta = 77.0$) or $\text{C}_6\text{D}_5\text{H}$ for ^1H ($\delta = 7.16$) and C_6D_6 itself for ^{13}C ($\delta = 128.0$). The absolute values of the coupling constants are given in Hertz (Hz). Multiplicities are abbreviated as singlet (s), doublet (d), triplet (t), septet (sep), multiplet (m), and broad (br). High-resolution mass spectroscopy measurements were performed on a Bruker micrOTOF II mass spectrometer with an atmospheric pressure chemical ionization (APCI) probe. Elemental analyses were performed on a Perkin Elmer 2400 series II CHN analyzer. Melting points were measured on a MPA100 Optimelt Automated Melting Point System and are uncorrected.

Synthesis of bismabenzene **1-Bi**

To a diethylether solution (20 mL) of aluminacyclohexadiene **2** (1.12 g, 1.88 mmol), BiCl_3 (1.48 g, 4.70 mmol) was added. After stirring at room temperature for 24 h, DBU was added to the mixture, and stirred for 77 h at room temperature. After evaporation of the solvent, hexane was added. The resulting suspension was filtered through a pad of Celite®. After removal of the solvent, recrystallization of the residual solid from hexane gave yellow crystals of bismabenzene **1-Bi** (266 mg, 0.454 mmol, 24%): mp (in a sealed tube) 122–125 °C (dec.); ^1H NMR (CDCl_3 , 500 MHz) δ : 1.14 (d, $J = 7$ Hz, 36H), 1.47 (sep, $J = 7$ Hz, 6H), 7.68 (t, $J = 9$ Hz, 1H), 11.62 (d, $J = 9$ Hz, 2H); ^{13}C NMR (CDCl_3 , 126 MHz) δ : 12.4 (CH_3), 19.1 (CH), 136.5 (CH, C_{meta}), 153.5 (CH, C_{para}), 222.4 (4°, C_{ortho}); ^1H NMR (C_6D_6 , 400 MHz) δ : 1.16 (d, $J = 7$ Hz, 36H), 1.40–1.48 (m, 6H), 7.87 (t, $J = 9$ Hz, 1H), 11.7 (d, $J = 9$ Hz, 2H); ^{13}C NMR (C_6D_6 , 100 MHz) δ : 12.6 (CH_3), 19.3 (CH), 137.2 (CH, C_{meta}), 154.3 (CH, C_{para}), 223.2 (4°, C_{ortho}); HRMS (APCI, positive) Calcd. For $\text{C}_{23}\text{H}_{45}\text{BiSi}_2$ [M⁺]: 586.2864. Found: 586.2854; Anal. calcd. for $\text{C}_{23}\text{H}_{45}\text{BiSi}_2$: C, 47.08; H, 7.73. Found C, 47.19; H, 8.04.

Observation of bismacyclohexadiene **3**

To a diethylether solution (10 mL) of aluminacyclohexadiene **2** (298 g, 0.500 mmol), BiCl_3 (394 mg, 1.25 mmol) was added. After stirring the reaction mixture at room temperature for 27 h, the mixture was concentrated under vacuum. The resulting mixture was dissolved in hexane and the hexane suspension was filtered through a pad of Celite®. After removal of the solvent from the filtrate, recrystallization of the residual solid gave crude bismacyclohexadiene **3** (98.8 mg, 0.159 mmol, 32%). Although the product could not be completely isolated, the

structure was confirmed by ^1H and ^{13}C NMR (Figure S1 and S2). The structure of **3** was also confirmed by X-ray crystallography using single crystals, which was afforded the recrystallization of crude product from hexane (Figure S3): ^1H NMR (C_6D_6 , 400 MHz) δ : 1.06 (d, $J = 6$ Hz, 18H), 1.11-1.20 (m, 24H), 3.39 (dt, $J = 19$ Hz, 7 Hz, 1H), 4.00 (dt, $J = 19$ Hz, 2 Hz, 1H), 8.13 (dd, $J = 7$ Hz, 2Hz 2H); ^{13}C NMR (C_6D_6 , 126 MHz) δ : 12.5 (CH), 19.0 (CH₃), 19.2 (CH₃), 66.7 (CH₂), 150.3 (CH), 166.9 (4°).

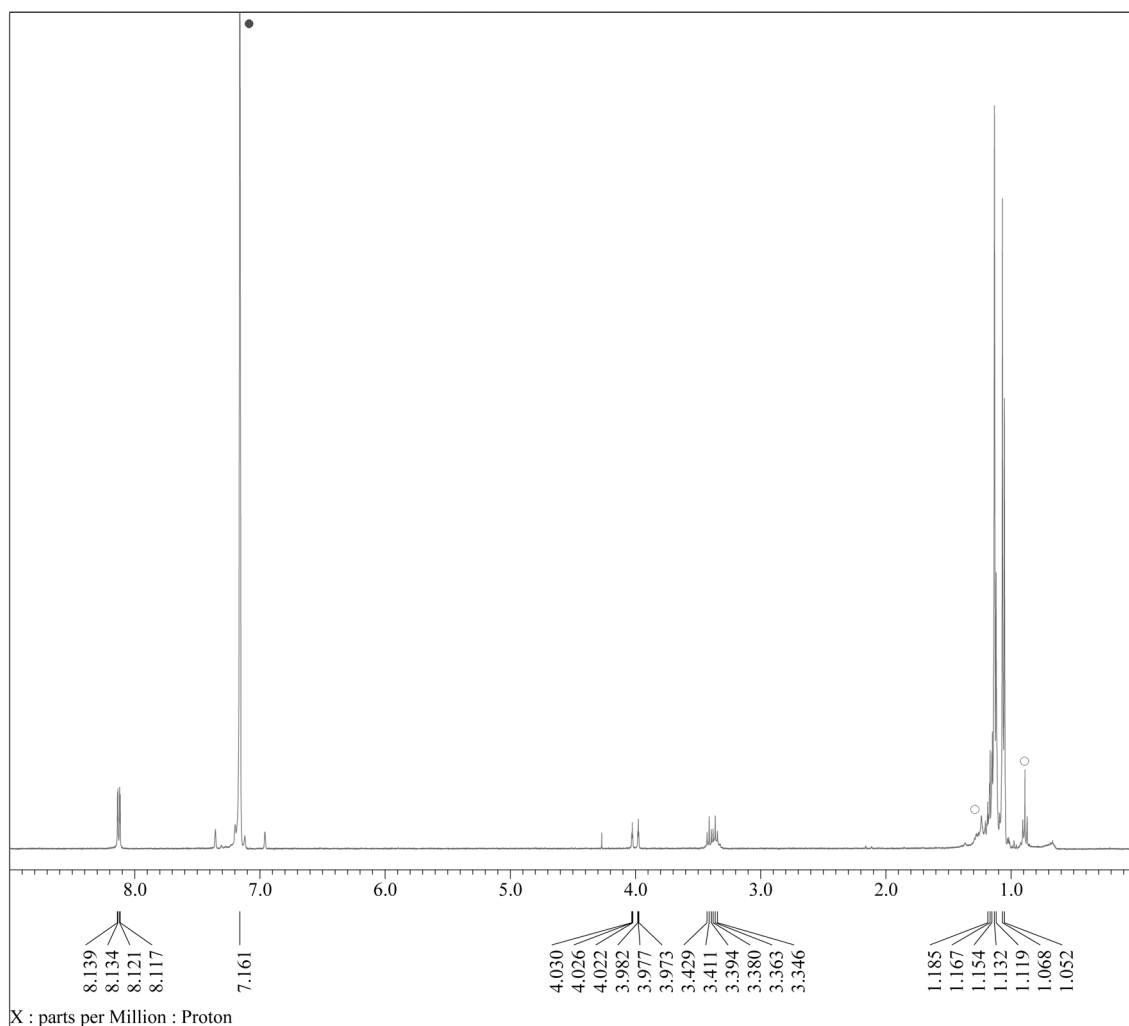


Figure S1. ^1H NMR spectrum of bismacyclohexadiene **3** in C_6D_6 (●: residual solvent signal, ○: hexane).

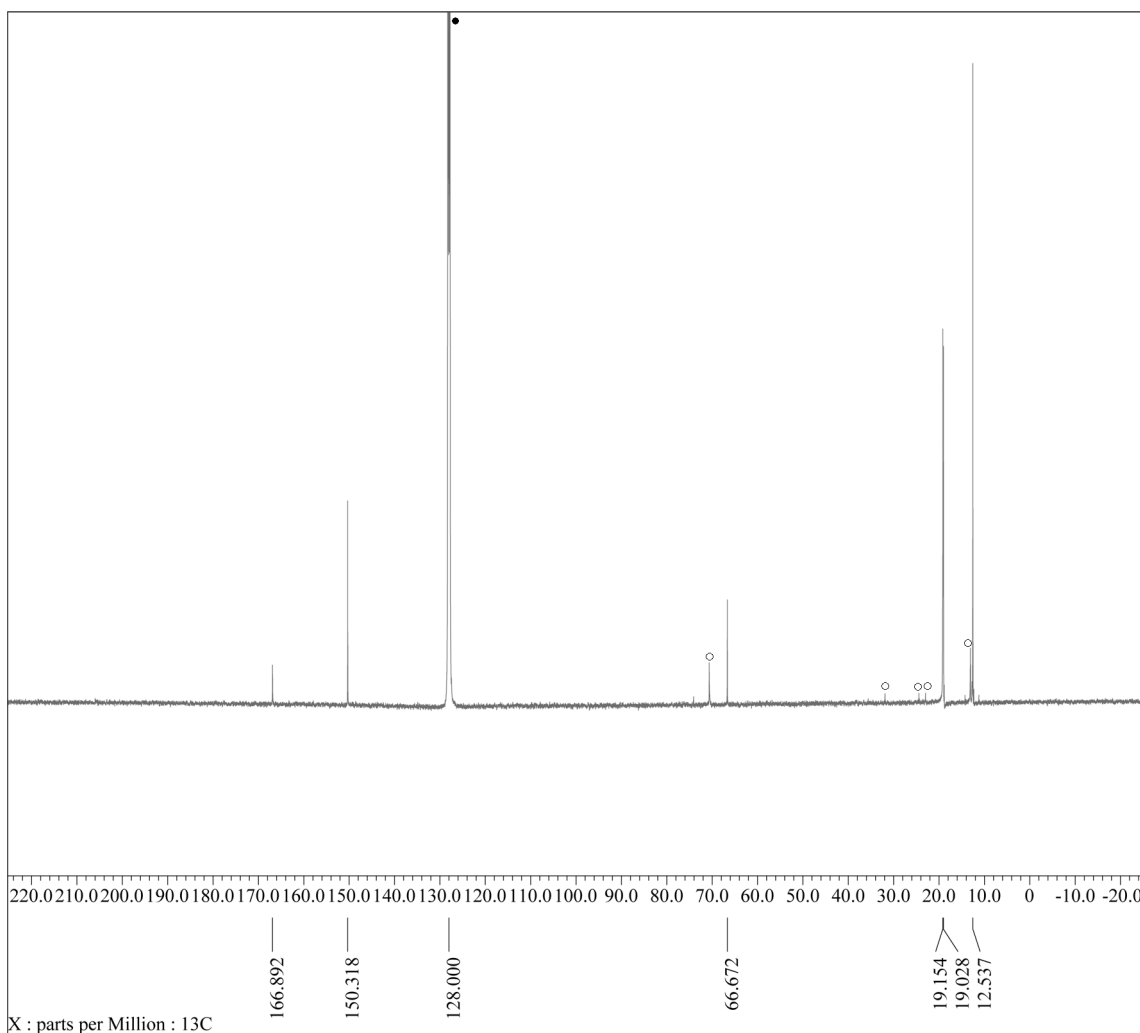


Figure S2. ^{13}C NMR spectrum of bismacyclohexadiene **3** in C_6D_6 (●: residual solvent signal, ○: impurities).

Reaction of bismabenzene **1-Bi** with DMAD

To a hexane solution (0.80 mL) of **1-Bi** (66.4 mg, 0.113 mmol), DMAD (13.4 μl , 0.114 mmol) was added. After stirring for 4 h at 70 °C, the resulting mixture was concentrated under vacuum. Hexane was added to the residue, and the resulting solution was filtered through Celite®. After evaporation of the solvent, DMAD adduct **4** was crystallized as colorless solid (82.0 mg, 0.113 mmol, 100%): mp (in a sealed tube) 82–84 °C (dec.); ^1H NMR (C_6D_6 , 400 MHz) δ : 0.99 (d, J = 6 Hz, 18H), 1.08 (d, J = 6 Hz, 18H), 1.05–1.15 (m, 6H), 3.31 (s, 3H), 3.50 (s 3H), 7.07 (t, J = 8 Hz, 1H), 8.36 (d, J = 8 Hz, 2H); ^{13}C NMR (C_6D_6 , 100 MHz) δ : 12.8 (CH_3), 19.2 (CH), 51.5 (CH_3), 52.1 (CH_3), 97.1 (CH), 139.4 (4°), 148.7 (CH), 160.3 (4°), 164.9 (4°) 165.6 (4°), 173.1 (4°); Anal. calcd. for $\text{C}_{29}\text{H}_{51}\text{BiO}_4\text{Si}_2$: C, 47.79; H, 7.05. Found C, 47.98; H, 7.28.

2. X-ray Crystallographic Analysis

Crystallographic data for **1-Bi**, **3** and **4** are summarized in Table S1. The crystal was coated with oil (Immersion Oil, type B: Code 1248, Cargille Laboratories, Inc.) and put on a MicroMountTM (MiTeGen, LLC), and then mounted on diffractometer. Diffraction data were collected on a Saturn CCD detectors using MoK α radiation. The Bragg spots were integrated using the CrystalClear program package.^{S2} Absorption corrections were applied. All the following procedure for analysis, Yadokari-XG 2009 was used as a graphical interface.^{S3} The structures were solved by a direct method with programs of SIR-97^{S4} or SIR2004^{S5} and refined by a full-matrix least squares method with the program of SHELXL-2013.^{S6} Anisotropic temperature factors were applied to all non-hydrogen atoms. The hydrogen atoms were put at calculated positions, and refined applying riding models.

Table S1. Crystallographic data for **1-Bi**, **3**, and **4**.

	1-Bi	3	4
formula	C ₂₃ H ₄₅ BiSi ₂	C ₂₃ H ₄₆ BiSi ₂	C ₂₉ H ₅₁ BiO ₄ Si ₂
<i>M</i>	586.75	623.21	728.85
<i>T</i> / K	93	93	93
color	yellow	pale-yellow	colorless
size, mm	0.20 x 0.09 x 0.06	0.14 x 0.13 x 0.07	0.12 x 0.09 x 0.09
crystal system	Monoclinic	Orthorhombic	Monoclinic
space group	<i>P</i> 2 ₁ /c (#14)	<i>P</i> nma (#62)	<i>P</i> 2 ₁ /n (#14)
<i>a</i> / Å	14.653(2)	12.556(7)	8.0332(12)
<i>b</i> / Å	12.2834(16)	226.674(15)	16.222(2)
<i>c</i> / Å	14.7811(19)	8.038(4)	25.418(4)
α / °	90	90	90
β / °	99.5679(19)	90	95.791(2)
γ / °	90	90	90
<i>V</i> / Å ³	2623.4(6)	2692(2)	3295.4(9)
<i>Z</i>	4	4	4
<i>D</i> _x / g cm ⁻³	1.486	1.538	1.469
μ / mm ⁻¹	6.818	6.744	5.452
<i>F</i> (000)	1176	1248	1472
θ range / °	3.25 to 27.49	3.01 to 27.50	3.02 to 27.48
reflections collected	21156	20877	26197
unique reflections	5862	3165	7534
refined parameters	247	133	339
GOF on <i>F</i> ²	1.035	1.099	1.101
<i>R</i> 1 [<i>I</i> > 2σ(<i>I</i>)] ^a	0.0303	0.0385	0.0571
w <i>R</i> 2 (all data) ^b	0.0716	0.0911	0.1971
$\Delta\rho_{\min, \max}$ / e Å ⁻³	-2.641, 0.781	-2.140, 1.695	-3.625, 6.430

^a *R*1 = Σ ||*F*_o| - |*F*_c|| / Σ |*F*_o|, ^b w*R*2 = [Σ {w(*F*_o² - *F*_c²)² / Σ w(*F*_o²)²}]^{1/2}

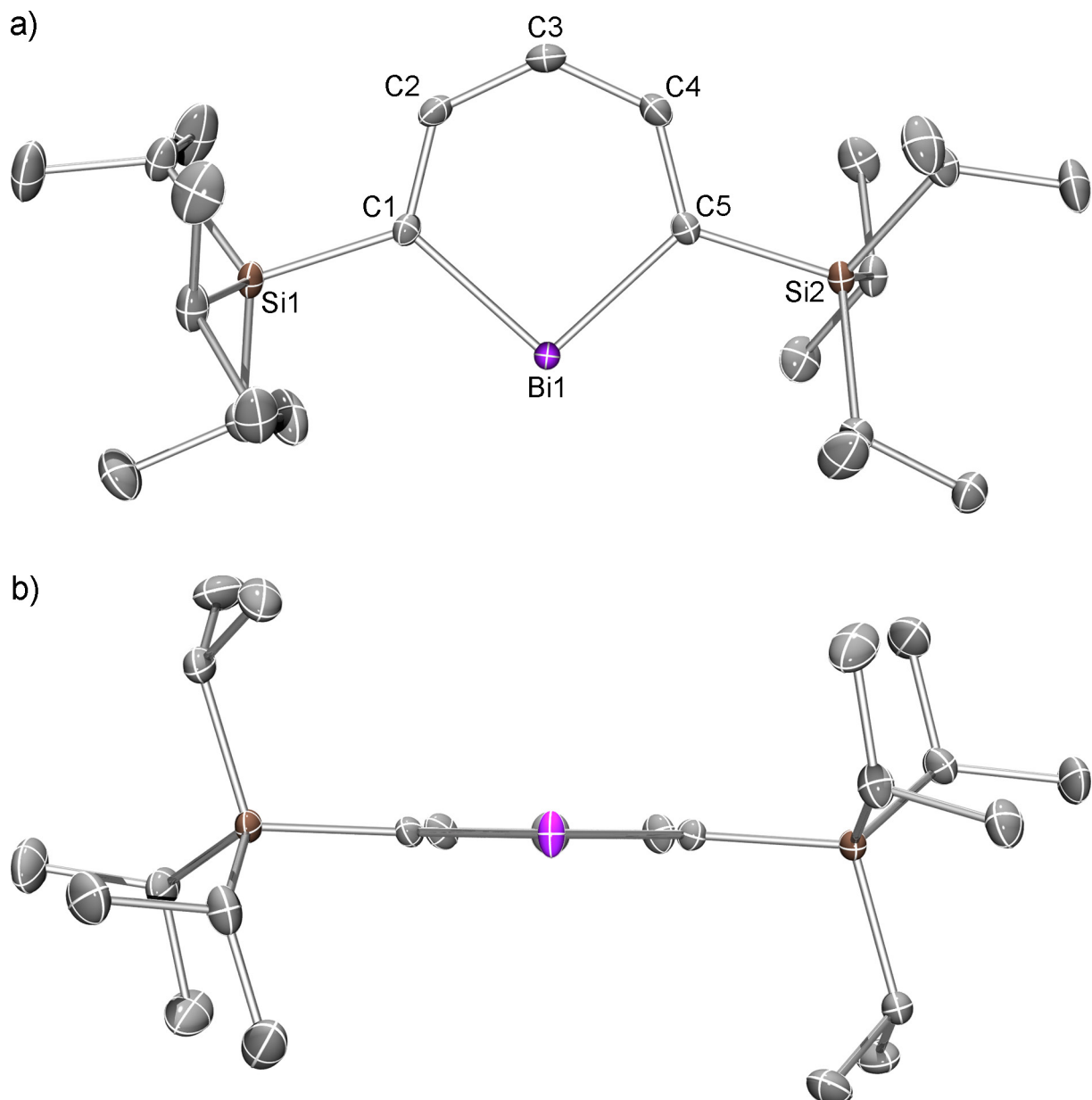
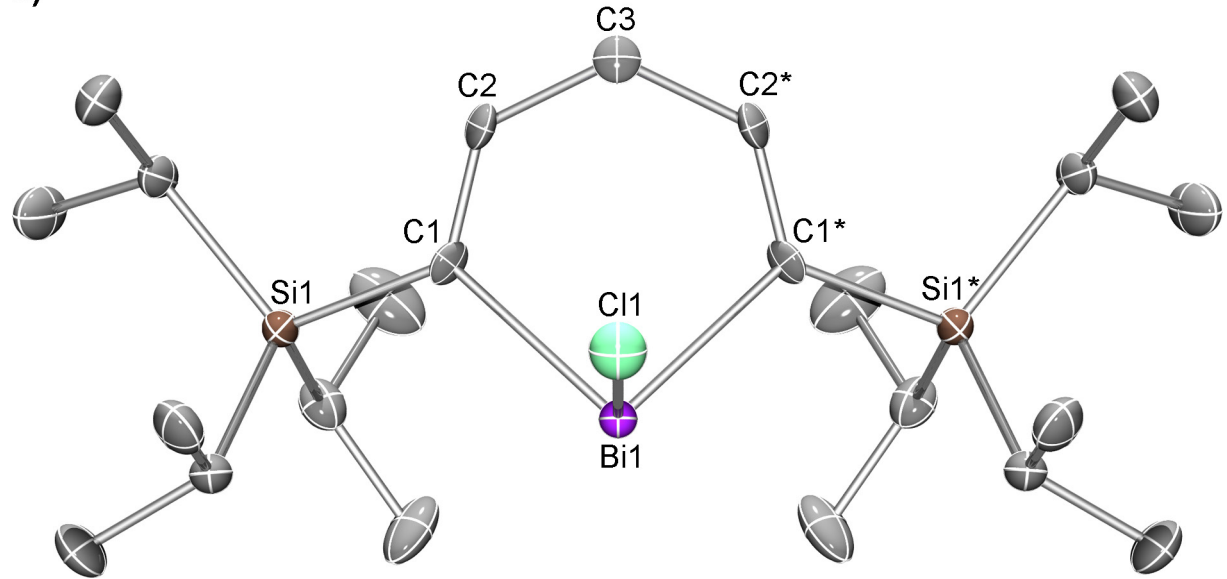


Figure S3. a) Molecular structure of **1-Bi** (50% thermal ellipsoid probability). Hydrogen atoms are omitted for clarity. b) Side view of **1-Bi**. Selected bond distances (\AA) and angles ($^\circ$) for **1-Bi**: Bi1–C1 = 2.160(4), Bi1–C5 = 2.154(4), C1–C2 = 1.398(5), C2–C3 = 1.402(6), C3–C4 = 1.393(6), C4–C5 = 1.395(6), C1–Si1 = 1.873(4), C5–Si2 = 1.876(4), C1–Bi1–C5 = 95.32(14), Bi1–C1–C2 = 118.4(3), C1–C2–C3 = 129.2(4), C2–C3–C4 = 128.9(4), C3–C4–C5 = 129.5(4), C4–C5–Bi1 = 118.6(3), Bi1–C1–Si1 = 120.04(19), Si1–C1–C2 = 121.5 (3), Bi1–C5–Si2 = 119.72(19), Si1–C1–C2 = 121.6 (3).

a)



b)

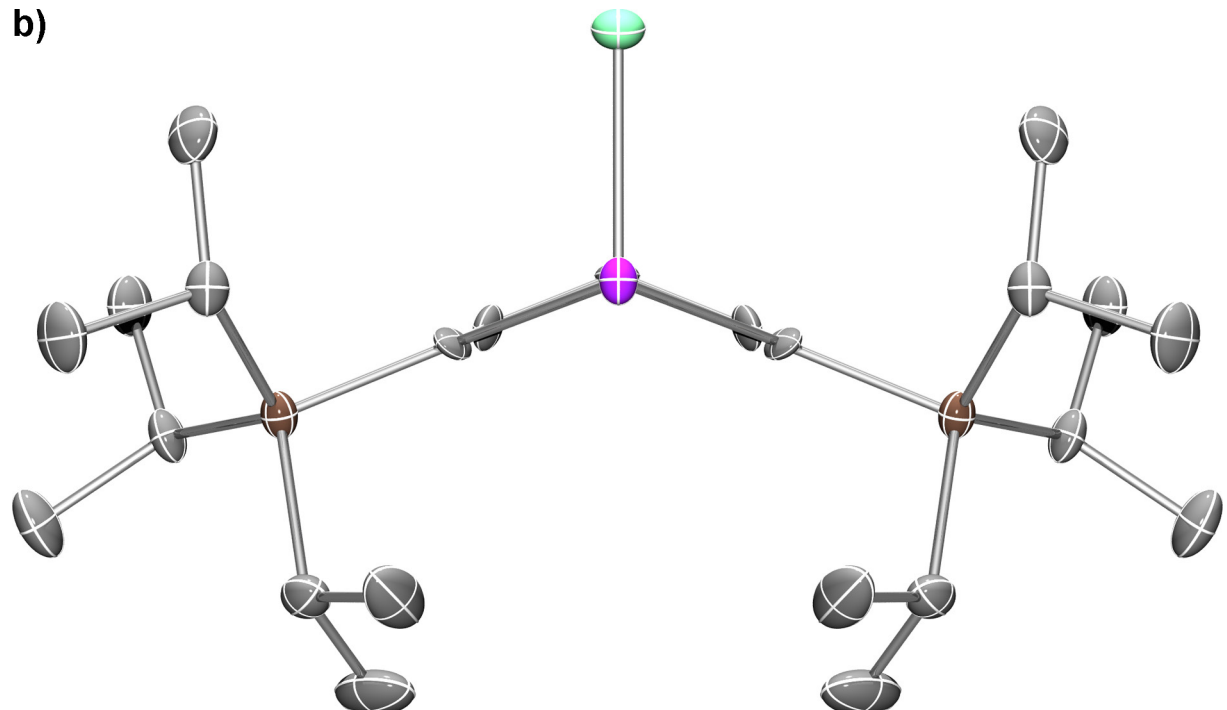


Figure S4. a) Molecular structure of **3** (50% thermal ellipsoid probability). Hydrogen atoms are omitted for clarity. Selected bond distances (\AA) and angles ($^\circ$) for **3**: Bi1–C1 = 2.243(4), Bi1–Cl1 = 2.501(2), C1–C2 = 1.334(6), C2–C3 = 1.511(5), C1–Si1 = 1.877(5), C1–Bi1–C1* = 90.6(2), C1–Bi1–Cl1 = 94.30(12), Bi1–C1–C2 = 115.6(3), C1–C2–C3 = 128.8(5), C2–C3–C2* = 116.1(5), Bi1–C1–Si1 = 119.8(2), Si1–C1–C2 = 124.6(3).

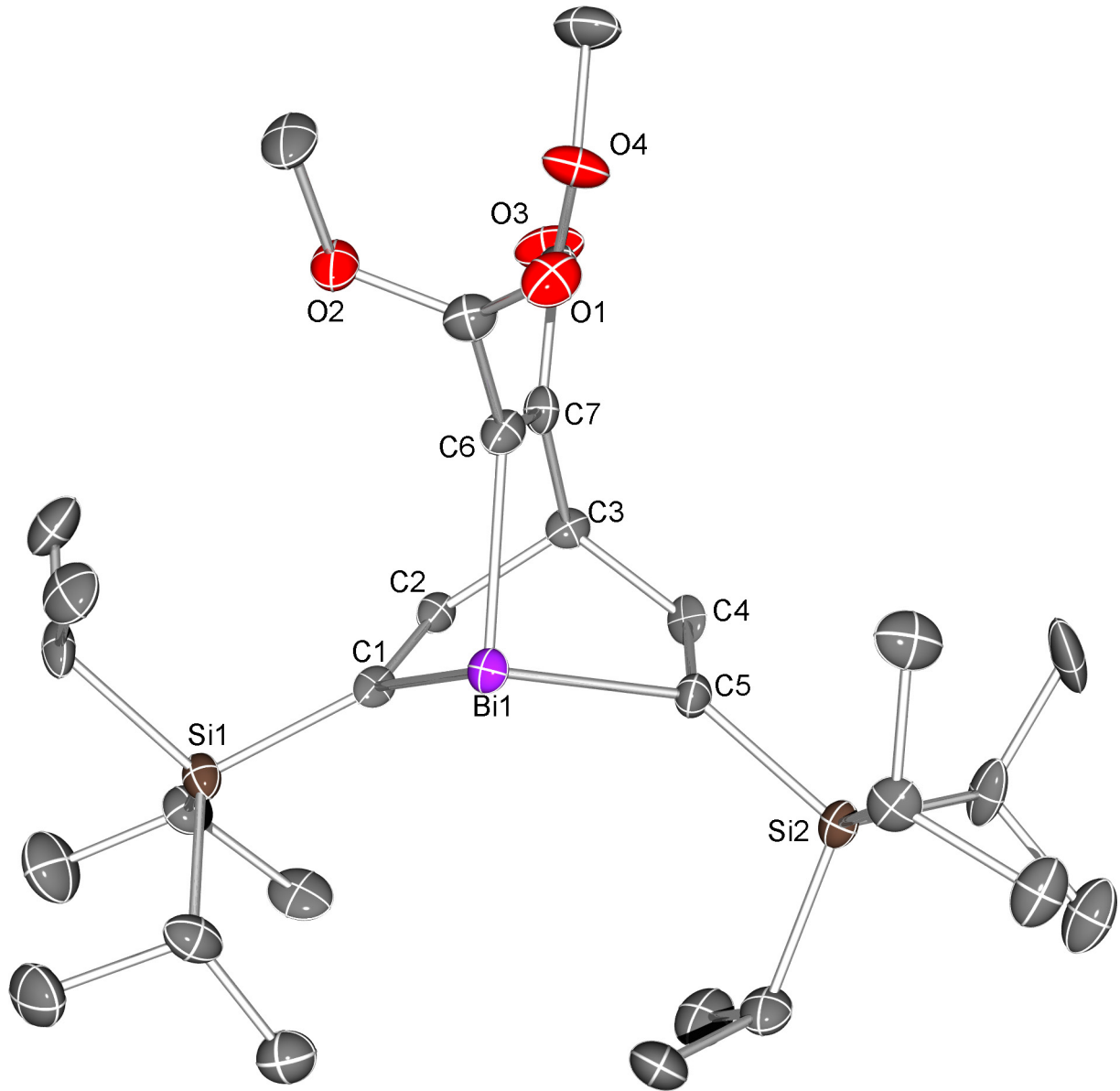


Figure S5. a) Molecular structure of DMAD-adduct **4** (50% thermal ellipsoid probability). Hydrogen atoms are omitted for clarity. Selected bond distances (\AA) and angles ($^\circ$) for **4**: $\text{Bi1-C1} = 2.265(9)$, $\text{Bi1-C5} = 2.274(11)$, $\text{Bi1-C6} = 2.273(10)$, $\text{C1-C2} = 1.322(13)$, $\text{C2-C3} = 1.530(14)$, $\text{C1-Si1} = 1.881(10)$, $\text{C3-C4} = 1.522(13)$, $\text{C4-C5} = 1.329(13)$, $\text{C6-C7} = 1.337(13)$, $\text{C4-C5} = 1.531(13)$, $\text{C1-Bi1-C5} = 87.3(4)$, $\text{C1-Bi1-C6} = 85.4(3)$, $\text{C5-Bi1-C6} = 86.9(4)$, $\text{Bi1-C1-C2} = 111.8(7)$, $\text{C1-C2-C3} = 125.4(9)$, $\text{C2-C3-C4} = 110.4(8)$, $\text{C3-C4-C5} = 125.6(9)$, $\text{Bi1-C5-C4} = 111.3(7)$, $\text{Bi1-C6-C7} = 113.7(7)$, $\text{C6-C7-C3} = 122.2(9)$.

3. UV-vis absorption spectrum

UV-vis absorption spectrum of **1-Bi** was recorded on a Shimadzu UV-3600 spectrometer with a resolution of 0.1 nm (Figure S6). 25.1 μ M of sample solution in a 1 cm square quartz cell was used for the measurement. Dry hexane was used for the sample solution.

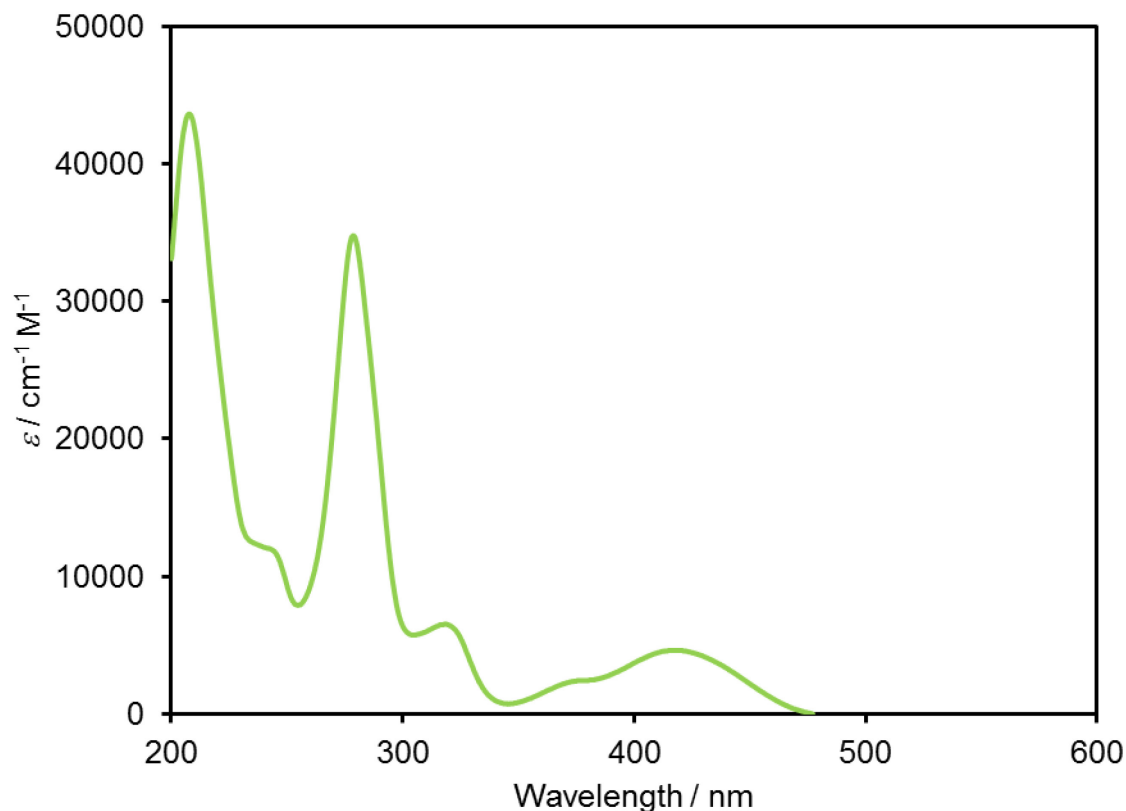


Figure S6. UV-vis absorption spectrum of **1-Bi** in hexane at room temperature. **1-Bi:** UV-vis (hexane) λ_{\max} (ε) = 417 nm ($4600 \text{ cm}^{-1} \text{M}^{-1}$), 375 nm (sh, $2400 \text{ cm}^{-1} \text{M}^{-1}$), 318 nm ($6500 \text{ cm}^{-1} \text{M}^{-1}$), 278 nm ($35000 \text{ cm}^{-1} \text{M}^{-1}$), 240 nm (sh, $12000 \text{ cm}^{-1} \text{M}^{-1}$), 208 nm ($44000 \text{ cm}^{-1} \text{M}^{-1}$).

4. Theoretical Calculations

All calculations were carried out by using ADF2016.102 program package.^{S7} The geometry optimization and frequency analysis of **1-Bi**, pyridine, 2,6-bis(*tri-iso-propylsilyl*)pyridine **1-N** were performed at the BP/TZ2P^{S8,S9} level of theory with scalar zeroth-order regular approximation (ZORA).^{S10} The optimized structures, selected structural parameters, and selected molecular orbitals of **1-Bi**, pyridine, and **1-N** are shown in Figure S7-S10. The Wiberg bond index (WBI)^{S11} were calculated by natural bond orbital (NBO) method (Figure S11).^{S12} The NICS values^{S13} and NMR chemical shifts were estimated using gauge-independent atomic orbital (GIAO) method^{S14} at the B3LYP/[QZ4P for Bi, Si, C, TZ2P for H]/BP/ TZ2P^{S9,S15} level of theory with the spin-orbit ZORA (Table S2 and Figure S12).^{S16} Time-dependent DFT calculation was carried out at the B3LYP/[QZ4P for Bi, Si, C, TZ2P for H]/BP/TZ2P^{S9,S15} level of theory with scalar ZORA (Table S3 and S4, Figure S13).

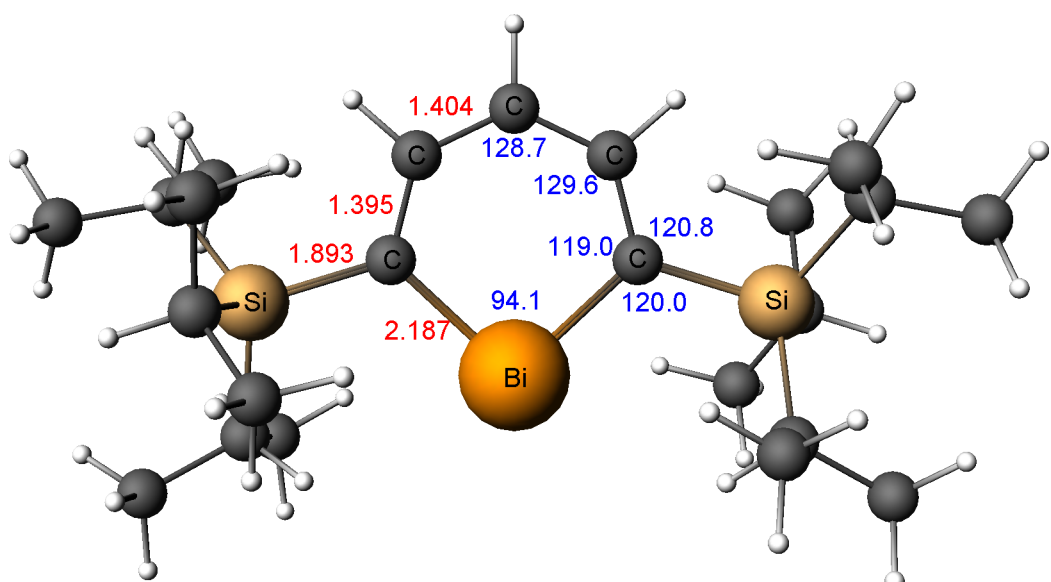


Figure S7. Optimized structure (C_2 symmetry) and selected bond distances (Å, Red) and angles (°, Blue) of **1-Bi** at the BP/TZ2P with scalar ZORA.

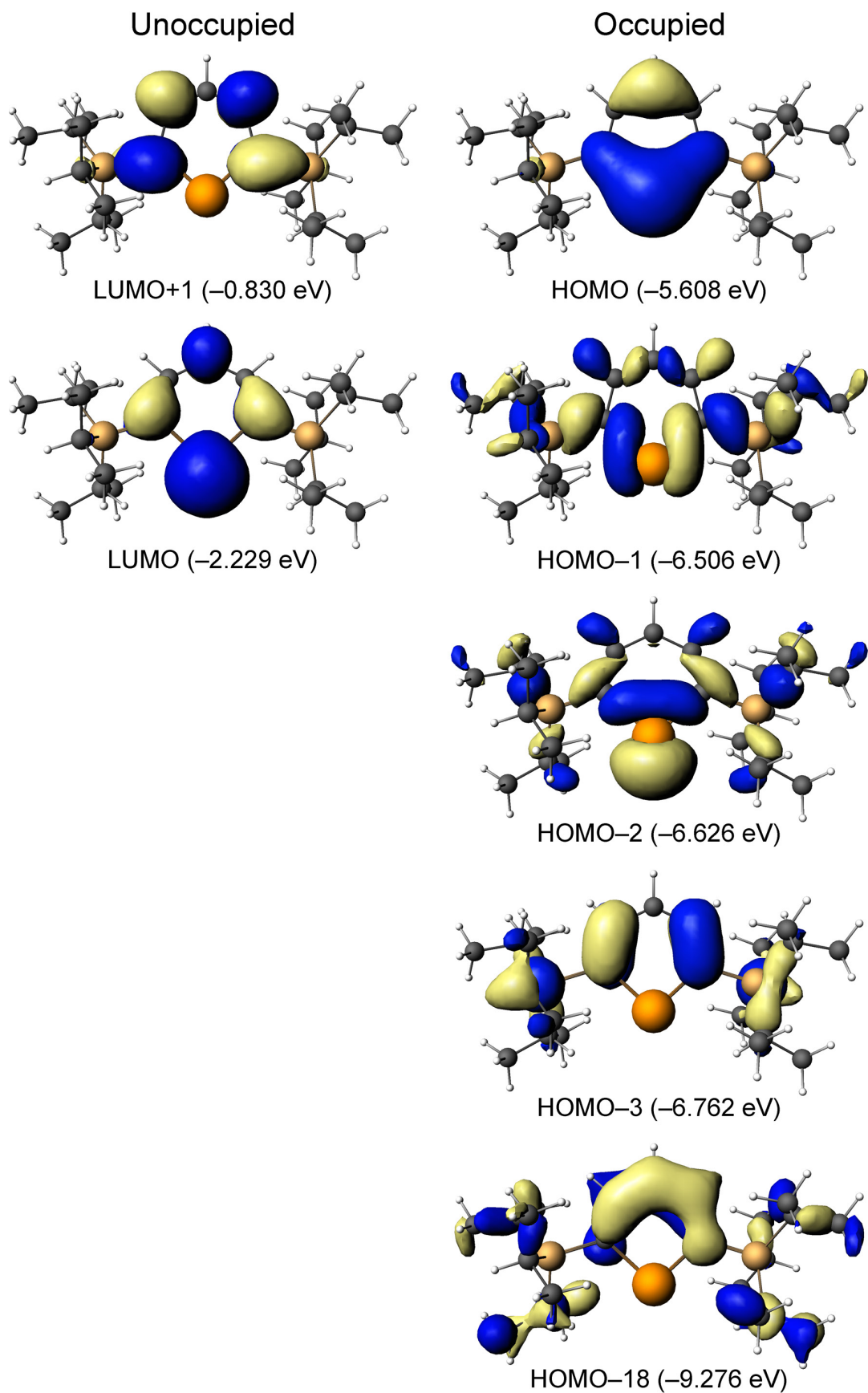


Figure S8. Frontier molecular orbitals of **1-Bi** calculated at the B3LYP/[QZ4P for Bi, Si, C, TZ2P for H]//BP/TZ2P with scalar ZORA.

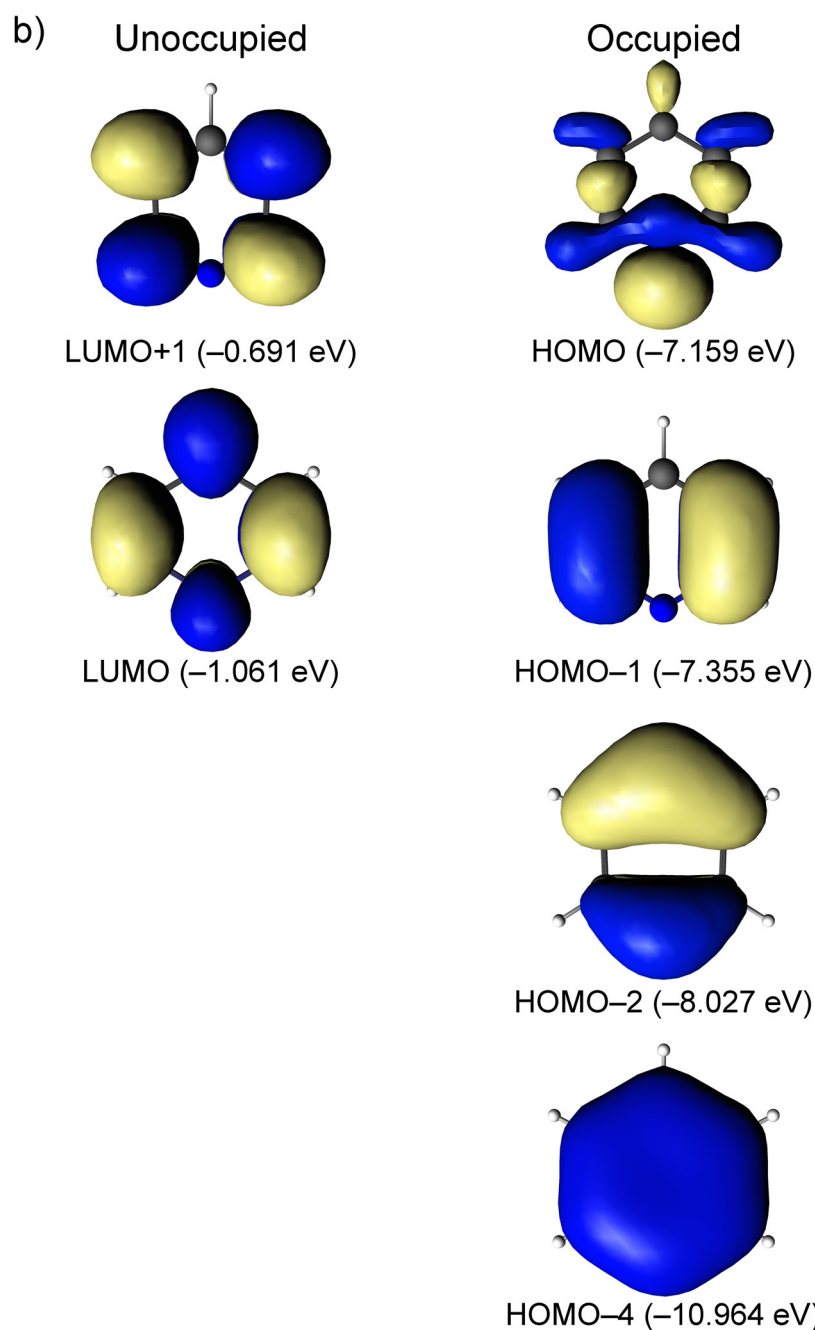
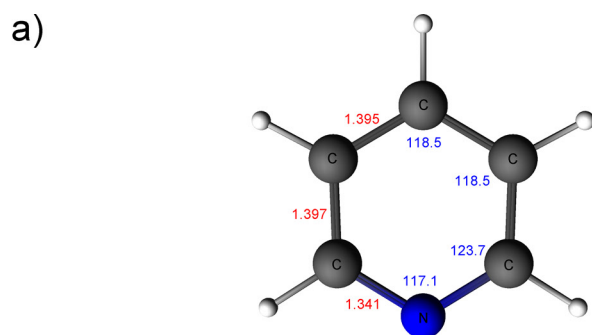


Figure S9. (a) Optimized Structure of pyridine at BP/TZ2P with scalar ZORA and (b) selected frontier molecular orbitals of pyridine calculated at the B3LYP/[QZ4P for N, C, TZ2P for H]//BP/TZ2P with scalar ZORA.

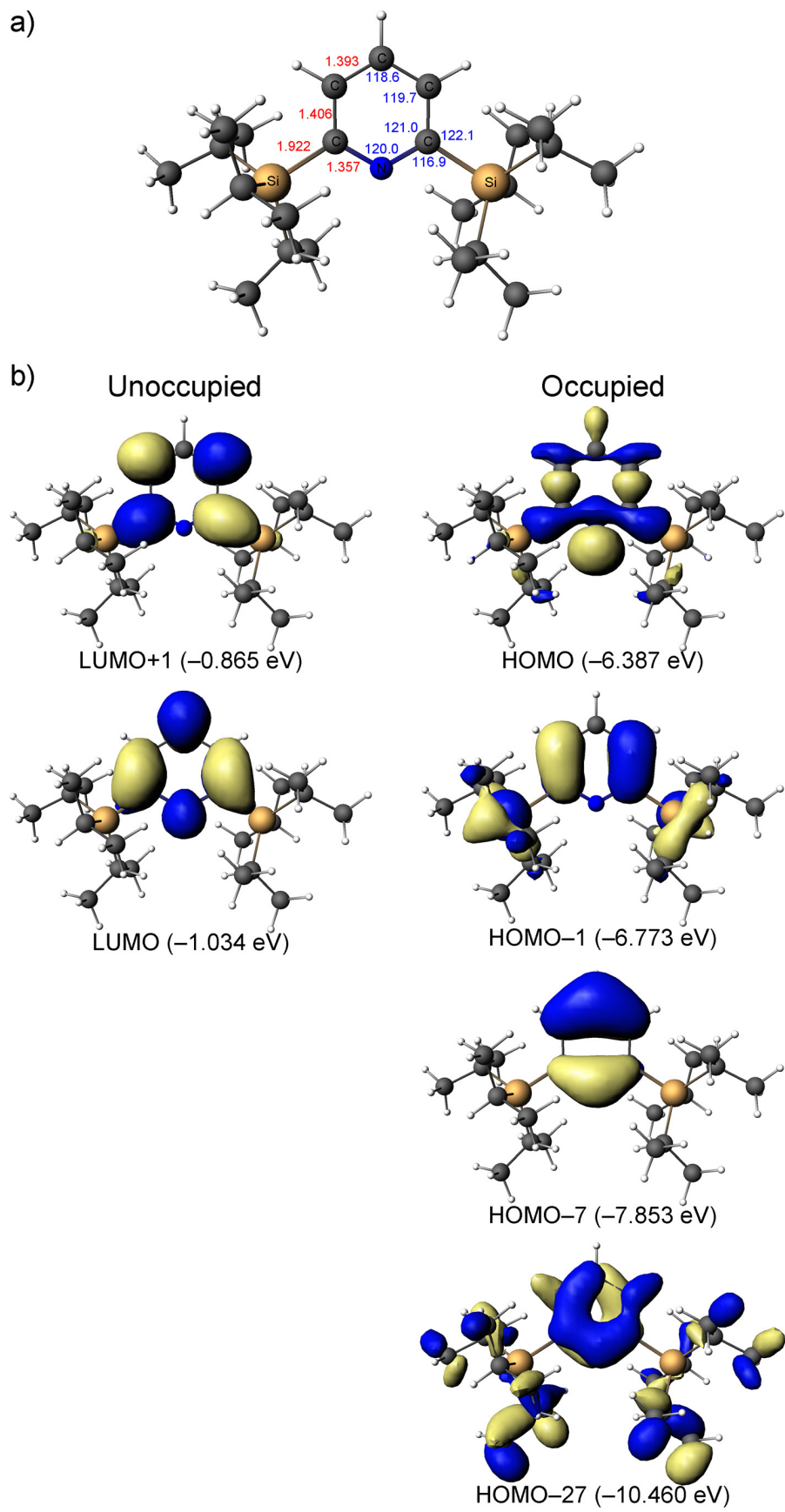


Figure S10. (a) Optimized Structure of **1-N** at BP/TZ2P with scalar ZORA and (b) selected frontier molecular orbitals of **1-N** calculated at the B3LYP/[QZ4P for N, C, TZ2P for H]//BP/TZ2P with scalar ZORA.

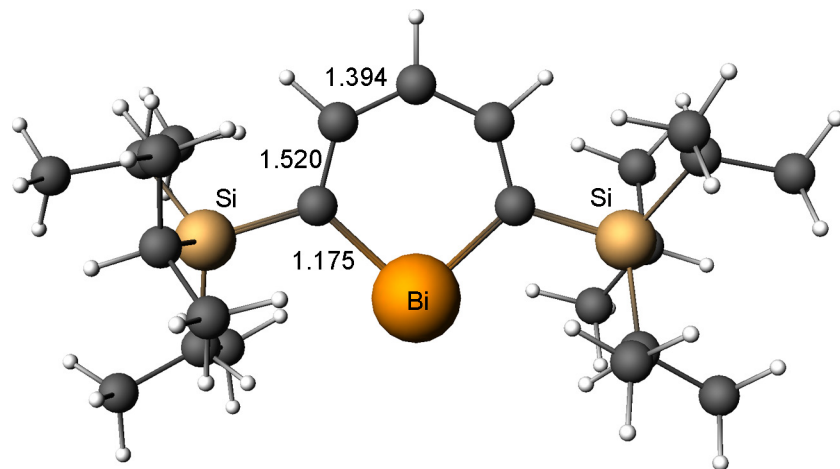


Figure S11. Wiberg bond induces (WBI) of **1-Bi** calculated at the B3LYP/[QZ4P for Bi, Si, C, TZ2P for H]/BP/TZ2P level with scalar ZORA.

Table S2. Calculated NICS values of **1-Bi**, pyridine, and **1-N** at the B3LYP/[QZ4P for Bi, Si, N, C, TZ2P for H]/BP/ TZ2P with spin-orbit ZORA.

	NICS(0)	NICS _{zz} (0)	NICS(1)	NICS _{zz} (1)
1-Bi	-3.4	-1.64	-7.3	-18.3
Pyridine	-6.5	-14.7	-9.9	-29.1
1-N	-4.5	-10.6	-9.5	-26.1

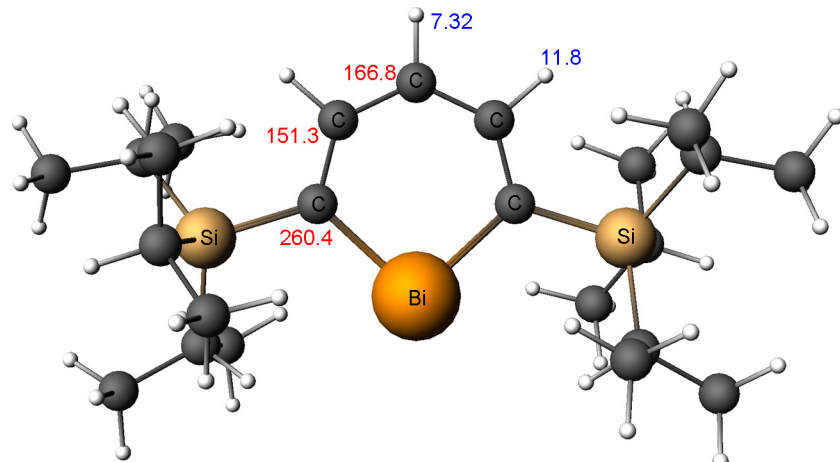


Figure S12. ¹H (Blue) and ¹³C NMR (Red) chemical shifts of **1-Bi** and pyridine at the B3LYP/[QZ4P for Bi, Si, C, TZ2P for H]/BP/TZ2P with spin-orbit ZORA.

Table S3. Transition energies of **1-Bi** predicted by TD-DFT calculations at the B3LYP/[QZ4P for Bi, Si, C, TZ2P for H]//BP/TZ2P with scalar ZORA.

Transition	Transition Energy <i>E/a.u.</i>	Transition Energy <i>E/eV</i>	Transition Energy <i>E/nm</i>	Oscillator Strength <i>f</i>
No.				
1	0.11886	3.2344	383.3347	5.31×10^{-2}
2	0.12056	3.2806	377.9286	9.20×10^{-3}
3	0.12766	3.4737	356.9248	3.11×10^{-3}
4	0.13787	3.7515	330.4886	4.14×10^{-3}
5	0.15649	4.2584	291.1544	0.30352
6	0.1571	4.275	290.0212	1.52×10^{-3}
7	0.15987	4.3503	285.0032	2.05×10^{-4}
8	0.16097	4.3801	283.0637	8.15×10^{-3}

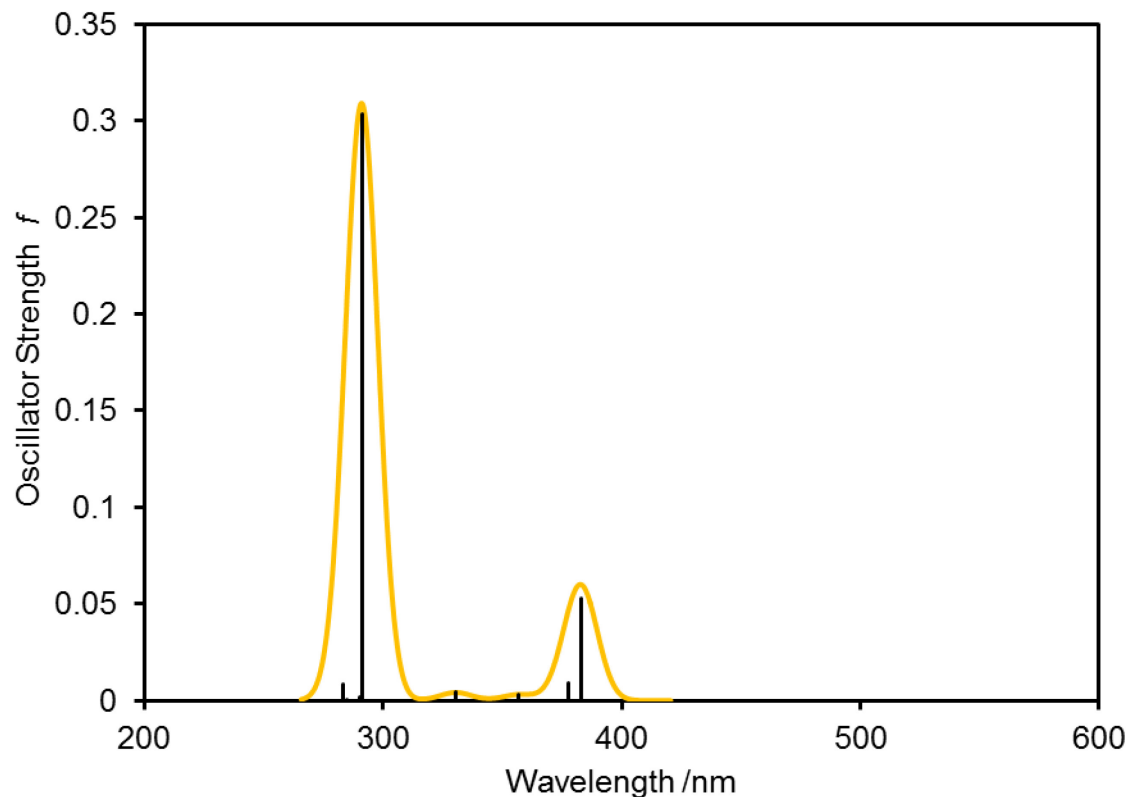


Figure S13. Simulated UV-vis absorption spectrum of **1-Bi** based on the eight electronic transitions calculated by TD-DFT calculation (Table S3).

Table S4. Selected contributions of MOs for the eight electronic transitions predicted by TD-DFT calculations at the B3LYP/[QZ4P for Bi, Si, C, TZ2P for H]//BP/TZ2P with scalar ZORA. Orbitals 147 and 148 are HOMO and LUMO.

Transition No.	Contributed MOs			Weight	Transition	Dipole	Moment
					x	y	z
1	147	->	148	0.7988	-2.2164	0	0
	146	->	148	0.1560	-0.0186	0	0
2	146	->	148	0.8209	-0.0425	0	0
	147	->	148	0.1521	0.9623	0	0
3	145	->	148	0.9594	0	-0.1919	-0.4603
	141	->	148	0.0304	0	-0.0107	-0.0266
4	144	->	148	0.6493	0	1.7638	0.1932
	147	->	149	0.3291	0	-1.6056	-0.0396
	140	->	148	0.0158	0	0.1044	-0.0429
5	147	->	149	0.4714	0	1.7539	0.0433
	144	->	148	0.3031	0	1.1187	0.1225
	140	->	148	0.1793	0	-0.3704	0.1521
	145	->	153	0.0109	0	-0.2356	0.0161
6	143	->	148	0.7954	0.1219	0	0
	142	->	148	0.1895	-0.2933	0	0
	146	->	148	0.0118	-0.0053	0	0
7	141	->	148	0.9555	0	0.0642	0.1595
	145	->	148	0.0309	0	-0.0368	-0.0883
8	142	->	148	0.7970	-0.5974	0	0
	143	->	148	0.1934	-0.0597	0	0

5. References

- (S1) Nakamura, T.; Suzuki, K.; Yamashita, M. *J. Am. Chem. Soc.* **2014**, *136*, 9276-9279.
- (S2) CrystalClear: Rigaku/MSC. Inc., 9009 New Trails Drive, The Woodlands TX 77381, USA (2005).
- (S3) Kabuto, C.; Akine, S.; Kwon, E. *J. Cryst. Soc. Jpn.* **2009**, *51*, 218-224.
- (S4) Altomare, A.; Burla, M. C.; Camalli, M.; Cascarano, G. L.; Giacovazzo, C.; Guagliardi, A.; Molterni, A. G. G.; Polidori, G.; Spagna, R. *J. Appl. Cryst.* **1999**, *32*, 115-119.
- (S5) Burla, M. C.; Caliandro, R.; Camalli, M.; Carrozzini, B.; Cascarano, G. L.; Caro, L. D.; Giacovazzo, C.; Polidori, G.; Spagna, R. *J. Appl. Cryst.* **2005**, *38*, 381-388.
- (S6) Sheldrick, G. M. *Acta Crystallogr. Sect. A* **2008**, *64*, 112-122.
- (S7) (a) Velde, G. t.; Bickelhaupt, F. M.; Baerends, E. J.; Guerra, F.; Gisbergen, S. J. A. v.; Snijders, J. G.; Ziegler, T. *J Compt. Chem.* **2001**, *22*, 931-967. (b) Guerra, C. F.; Snijders, J. G.; Velde, G. t.; Baerends, E. J. *Teor. Chem. Acc.* **1998**, *99*, 391-403. (c) Baerends, E. J.; Ziegler, T.; Atkins, A. J.; Autschbach, J.; Bashford, D.; Bérçes, A.; Bickelhaupt, F. M.; Bo, C.; Boerrigter, P. M.; Cavallo, L.; Chong, D. P.; Chulhai, D. V.; Deng, L.; Dickson, R. M.; Dieterich, J. M.; Ellis, D. E.; Faassen, M. v.; Fan, L.; Fischer, T. H.; Guerra, C. F.; Franchini, M.; Ghysels, A.; Giammona, A.; Gisbergen, S. J. A. v.; Götz, A. W.; Groeneveld, J. A.; Gritsenko, O. V.; Grüning, M.; Gusarov, S.; Harris, F. E.; Hoek, P. v. d.; Jacob, C. R.; Jacobsen, H.; Jensen, L.; Kaminski, J. W.; Kessel, G. v.; Kootstra, F.; Kovalenko, A.; Krykunov, M. V.; Lenthe, E. v.; McCormack, D. A.; Michalak, A.; Mitoraj, M.; Morton, S. M.; Neugebauer, J.; Nicu, V. P.; Noodleman, L.; Osinga, V. P.; Patchkovskii, S.; Pavanello, M.; Peeples, C. A.; Philipsen, P. H. T.; Post, D.; Pye, C. C.; Ravenek, W.; Rodríguez, J. I.; Ros, P.; Rüger, R.; Schipper, P. R. T.; Schoot, H. v.; Schreckenbach, G.; Seldenthuis, J. S.; Seth, M.; Snijders, J. G.; Solà, M.; Swart, M.; Swerhone, D.; Velde, G. t.; Verwoerijs, P.; Versluis, L.; Visscher, L.; Visser, O.; Wang, F.; Wesolowski, T. A.; Wezenbeek, E. M. v.; Wiesenecker, G.; Wolff, S. K.; Woo, T. K.; Yakovlev, A. L. ADF2016, SCM, Theoretical Chemistry, Vrije Universiteit, Amsterdam, The Netherlands, <https://www.scm.com>.
- (S8) (a) Becke, A. D. *Phys. Rev. A* **1988**, *38*, 3098-3100. (b) Perdew, J. P. *Phys. Rev. B* **1986**, *33*, 8822-8824.
- (S9) Lenthe, E. v.; Baerends, E. J. *J. Compt. Chem.* **2003**, *24*, 1142-1156.
- (S10) (a) Lenthe, E. v.; Baerends, E. J.; Snijders, J. G. *J. Chem. Phys.* **1993**, *99*, 4597-4610. (b) Lenthe, E. v.; Baerends, E. J.; Snijders, J. G. *J. Chem. Phys.* **1994**, *101*, 9783-9792. (c) Lenthe, E. v.; Ehlers, A.; Baerends, E. J. *J. Chem. Phys.* **1999**, *110*, 8943-8953.
- (S11) Sizova, O. V.; Skripnikov, L. V.; Sokolov, A. Y. *THEOCHEM* **2008**, *870*, 1-9.
- (S12) Reed, A. E.; Curtiss, L. A.; Weinhold, F. *Chem. Rev.* **1988**, *88*, 899-926.
- (S13) Chen, Z.; Wannere, C. S.; Corminboeuf, C.; Puchta, R.; Schleyer, P. v. R. *Chem. Rev.* **2005**, *105*, 3842-3888.
- (S14) (a) Schreckenbach, G.; Ziegler, T. *J. Chem. Phys.* **1995**, *99*, 606-611. (b) Krykunov, M.; Ziegler, T.; Lenthe, E. v. *Int. J. Quantum Chem.* **2009**, *109*, 1676-1683. (c) Wolff, S. K.; Ziegler, T. *J. Chem. Phys.* **1998**, *109*, 895-905. (d) Wolff, S. K.; Ziegler, T.; Lenthe, E. v.; Baerends, E. J. *J. Chem. Phys.* **1999**, *110*, 7689-7698.
- (S15) (a) Becke, A. D. *J. Chem. Phys.* **1993**, *98*, 5648-5652. (b) Lee, C.; Yang, W.; Parr, R. G. *Phys. Rev. B* **1988**, *37*, 785-789. (c) Miehlich, B.; Savin, A.; Stoll, H.; Preuss, H. *Chem. Phys. Lett.* **1989**, *157*, 200-206.
- (S16) Lenthe, E. v.; Snijders, J. G.; Baerends, E. J. *J. Chem. Phys.* **1996**, *105*, 6505-6516.
- (S17) (a) Gisbergen, S. J. A. v.; Snijders, J. G.; Baerends, E. J. *Comput. Phys. Chem.* **1999**, *118*, 119-138. (b) Rosa, A.; Baerends, E. J.; Gisbergen, S. J. A. v.; Lenthe, E. v.; Groeneveld, J. A.; Snijders, J. G. *J. Am. Chem. Soc.* **1999**, *121*, 10356-10365.